SUPPORTING INFORMATION

Title: Photolabile Ru Model Complexes with Chelating Diimine Ligands for Light-Triggered Drug Release
Author(s): Federica Battistin, Gabriele Balducci, Jianhua Wei, Anna K. Renfrew,* Enzo Alessio*

Figure S1. UV-vis spectra of compounds [Ru([9]aneS$_3$)(bpy)Cl]Cl (**1**), [Ru([9]aneS$_3$)(phen)Cl]Cl (**2**), [Ru([9]aneS$_3$)(4,7-Ph$_2$phen)Cl]Cl (**3**), [Ru([9]aneS$_3$)(dppz)Cl]Cl (**4**), [Ru([9]aneS$_3$)(bq)Cl]Cl (**5**) (ca. in 0.1 mM H_2O) in the visible region.

Figure S2. ^{1}H NMR spectrum (aromatic region) in D_2O of [Ru([9]aneS$_3$)(bpy)Cl]Cl (**1**), and [Ru([9]aneS$_3$)(bpy)(OH$_2$)]Cl$_2$ (**1$_{aq}$**).

Figure S3. Molecular structure (50% probability ellipsoids) of [Ru([9]aneS$_3$)(phen)(py)]Cl$_2$·EtOH (**7**).

Figure S4-7. ^{1}H NMR spectra in D_2O of [Ru([9]aneS$_3$)(bpy)(py)]Cl$_2$ (**6**), [Ru([9]aneS$_3$)(phen)(py)]Cl$_2$ (**7**), [Ru([9]aneS$_3$)(4,7-Ph$_2$phen)(py)]Cl$_2$ (**8**), [Ru([9]aneS$_3$)(dppz)(py)]Cl$_2$ (**9**).

Figure S8. UV-vis spectrum of [Ru([9]aneS$_3$)(dppz)]Cl$_2$ (**9**) (ca. in 0.1 mM H_2O) in between 450 and 600 nm.

Figure S9. ^{1}H NMR spectrum in DMSO-d_6 of [Ru([9]aneS$_3$)(bq)(py)]Cl$_2$ (**10**) after 240 min of irradiation (λ = 470 nm, 40 mW).

Figure S10. Experimental (top) and calculated (with the "turbo_lanczos" program, bottom) absorption spectra for complex **6**. The vertical bars in the simulated spectrum are the calculated transitions (with the "turbo_davidson" code), with height equal to the oscillator strength.

Figure S11. Selected molecular orbitals for **6** (right) and **10** (left) in the singlet ground state.

Figure S12. ^{1}H NMR spectrum in D_2O of [Ru([9]aneS$_3$)(bq)(py)]Cl$_2$ (**10**) at different irradiation times (λ = 470 nm, 40 mW).

Table S1. Selected TDDFT singlet transitions for complex **10**.

Table S2. Crystallographic data and refinement details for compounds [Ru([9]aneS$_3$)(phen)(py)]Cl$_2$·EtOH (**7**), [Ru([9]aneS$_3$)(bq)(py)]Cl$_2$ (**10**), *trans*-RuCl$_2$(bq)(CO)$_2$·2CHCl$_3$ (**11**), and [Ru([9]aneS$_3$)(bq)(NH$_3$)]Cl$_2$·CH$_3$OH (**12**).

Tables S3-S6. Selected coordination distances (Å) and angles (°) for compounds [Ru([9]aneS$_3$)(phen)(py)]Cl$_2$·EtOH (**7**), [Ru([9]aneS$_3$)(bq)(py)]Cl$_2$ (**10**), *trans*-RuCl$_2$(bq)(CO)$_2$·2CHCl$_3$ (**11**), and [Ru([9]aneS$_3$)(bq)(NH$_3$)]Cl$_2$·CH$_3$OH (**12**).

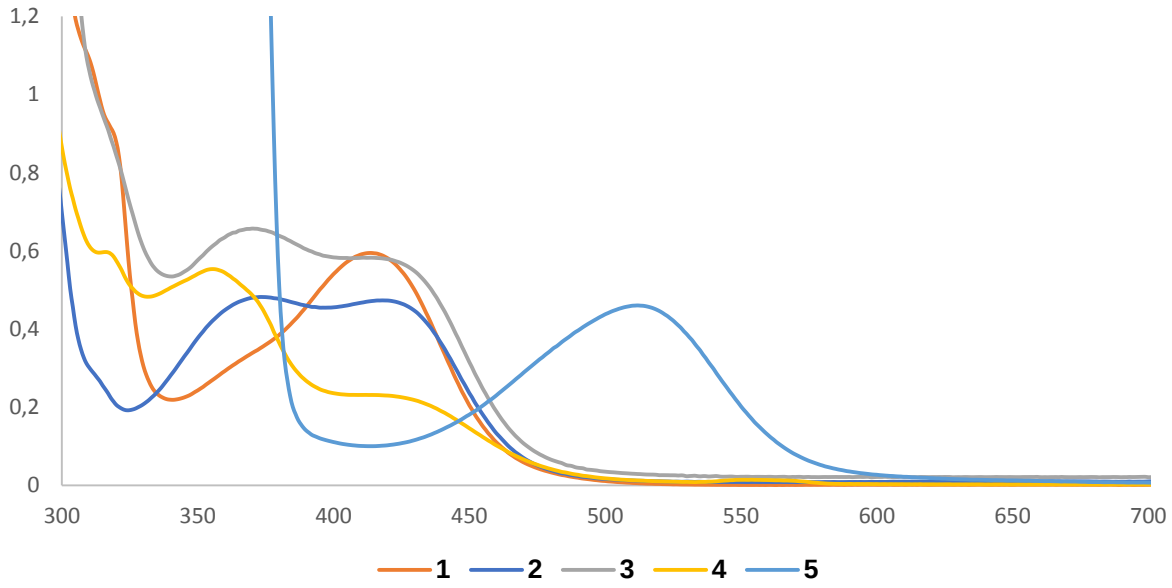

Figure S1. UV-vis spectra of [Ru([9]aneS$_3$)(bpy)Cl]Cl (**1**), [Ru([9]aneS$_3$)(phen)Cl]Cl (**2**), [Ru([9]aneS$_3$)(4,7-Ph$_2$phen)Cl]Cl (**3**), [Ru([9]aneS$_3$)(dppz)Cl]Cl (**4**), [Ru([9]aneS$_3$)(bq)Cl]Cl (**5**) (ca. in 0.1 mM H_2O) in the visible region.

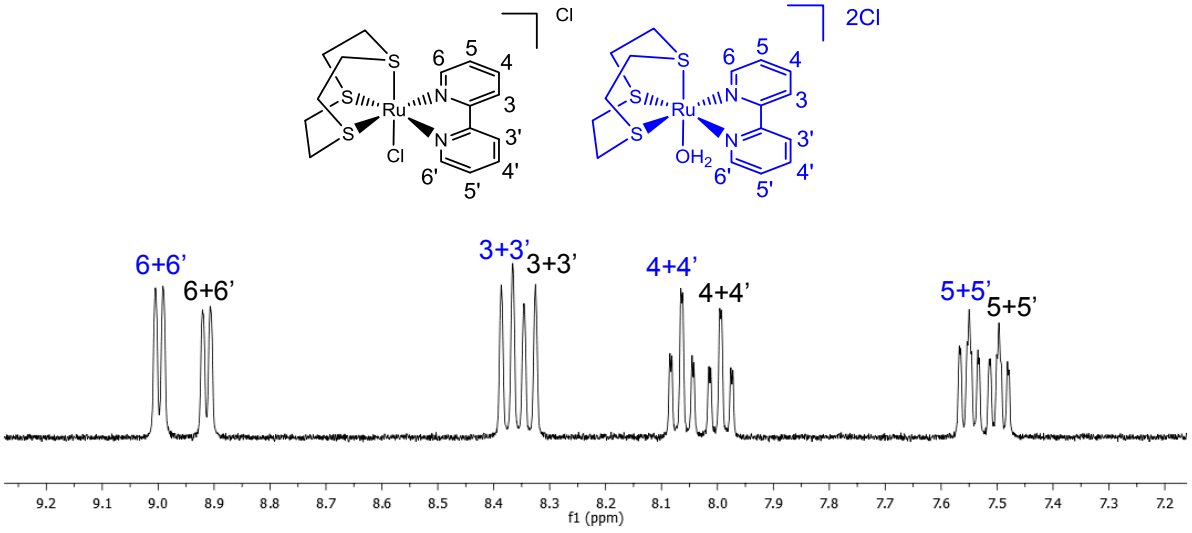

Figure S2. ^{1}H NMR spectrum (aromatic region) in D_2O of [Ru([9]aneS$_3$)(bpy)Cl]Cl (**1**), and [Ru([9]aneS$_3$)(bpy)(OH$_2$)]Cl$_2$ (**1$_{aq}$**).

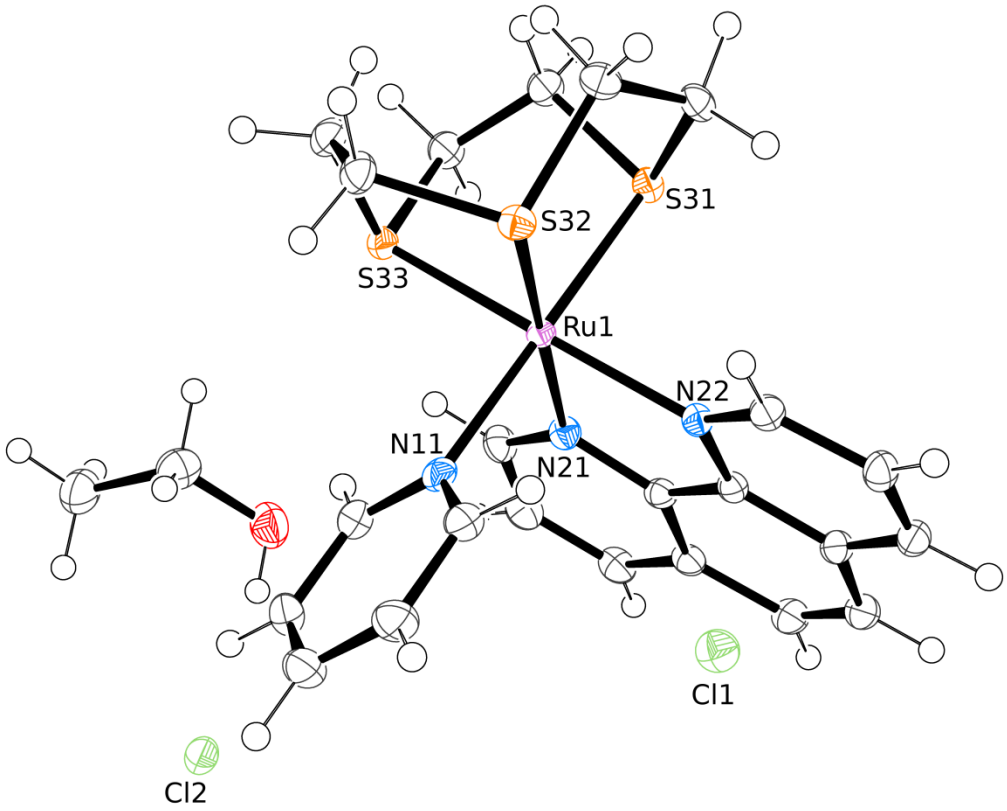

Figure S3. Molecular structure (50% probability ellipsoids) of [Ru([9]aneS$_3$)(phen)(py)]Cl$_2$·EtOH (**7**).

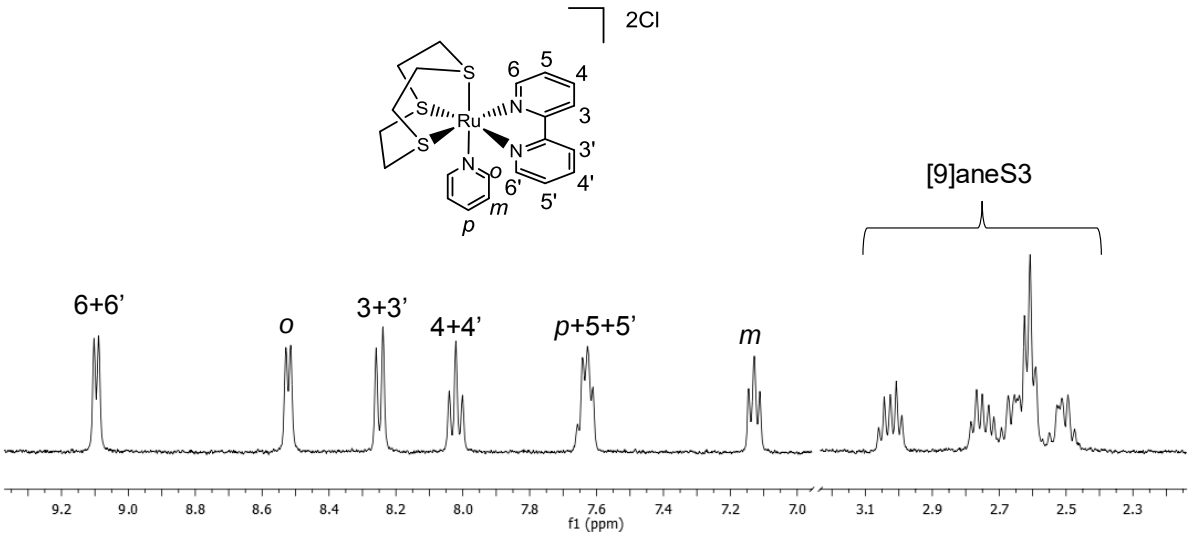

Figure S4. ^{1}H NMR spectrum in D$_2$O of [Ru([9]aneS$_3$)(bpy)(py)]Cl$_2$ (**6**).

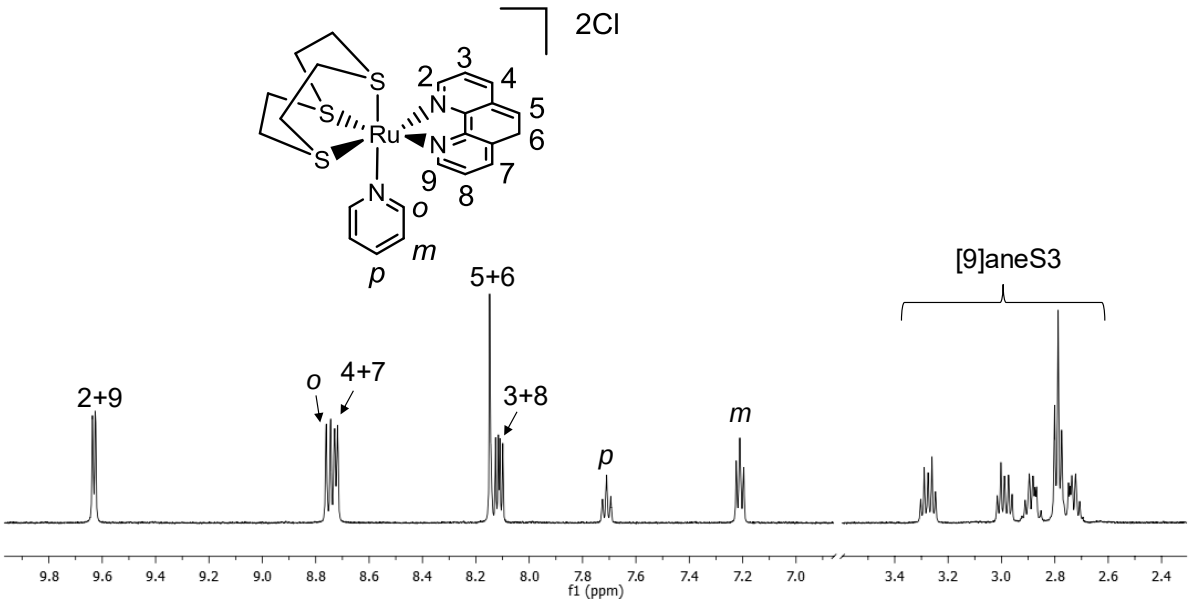

Figure S5. ^{1}H NMR spectrum in D_2O of [Ru([9]aneS_3)(phen)(py)]Cl_2 (**7**).

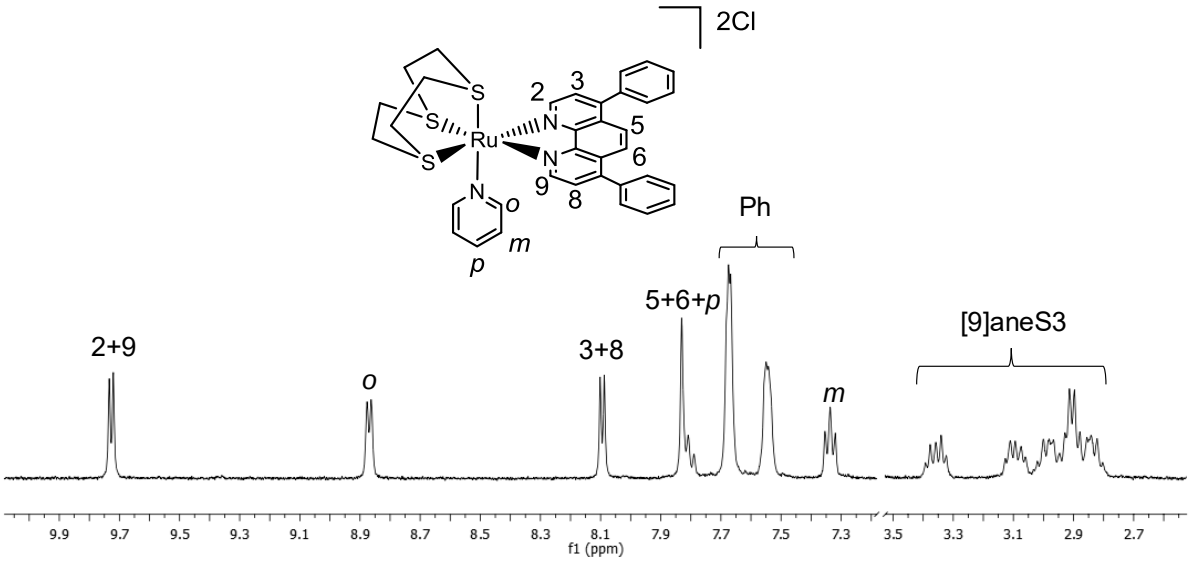

Figure S6. ^{1}H NMR spectrum in D_2O of [Ru([9]aneS_3)(4,7-Ph_2phen)(py)]Cl_2 (**8**).

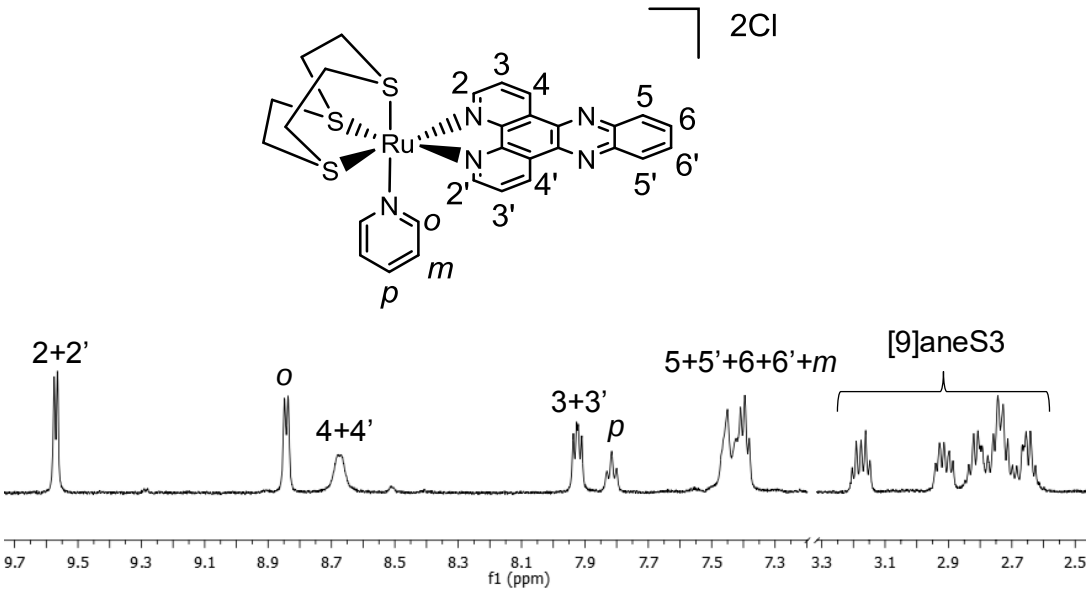

Figure S7. ^{1}H NMR spectrum in D_2O of [Ru([9]aneS_3)(dppz)(py)]Cl_2 (**9**).

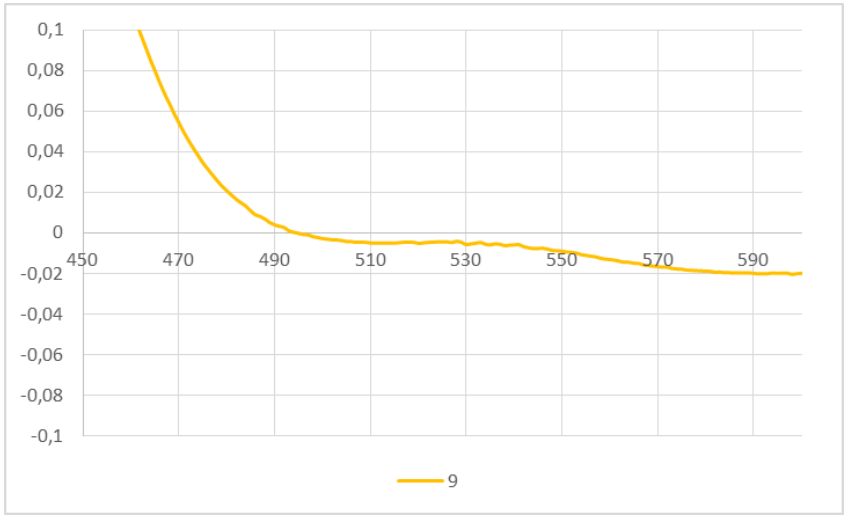

Figure S8. UV-vis spectrum of [Ru([9]aneS_3)(dppz)(py)]Cl_2 (**9**) (ca. in 0.1 mM H_2O) between 450 and 600 nm.

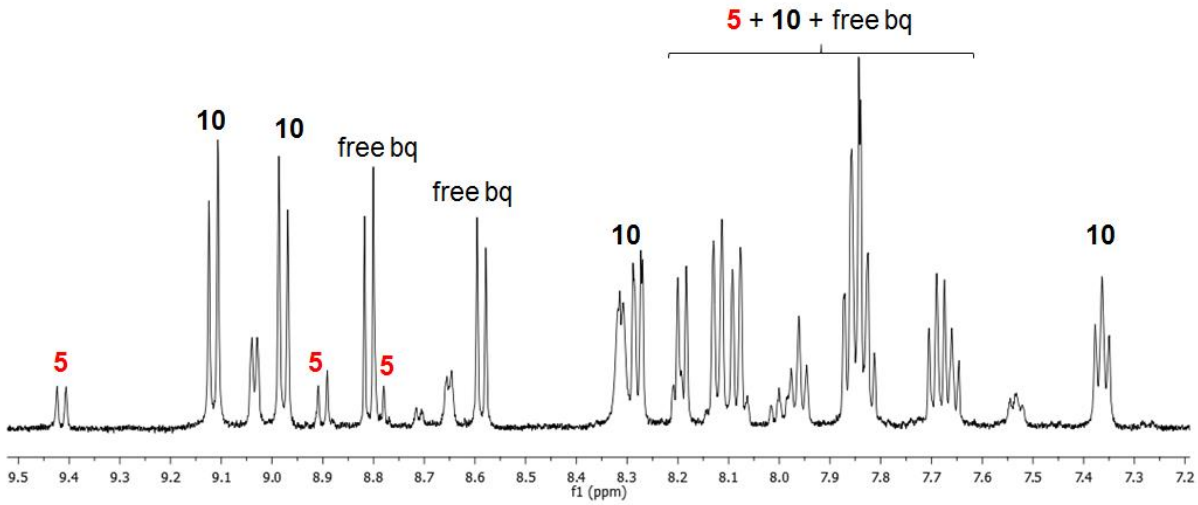

Figure S9. ^{1}H NMR spectrum in DMSO-d_6 of [Ru([9]aneS_3)(bq)(py)]Cl_2 (**10**) after 240 min of irradiation (λ = 470 nm, 40 mW).

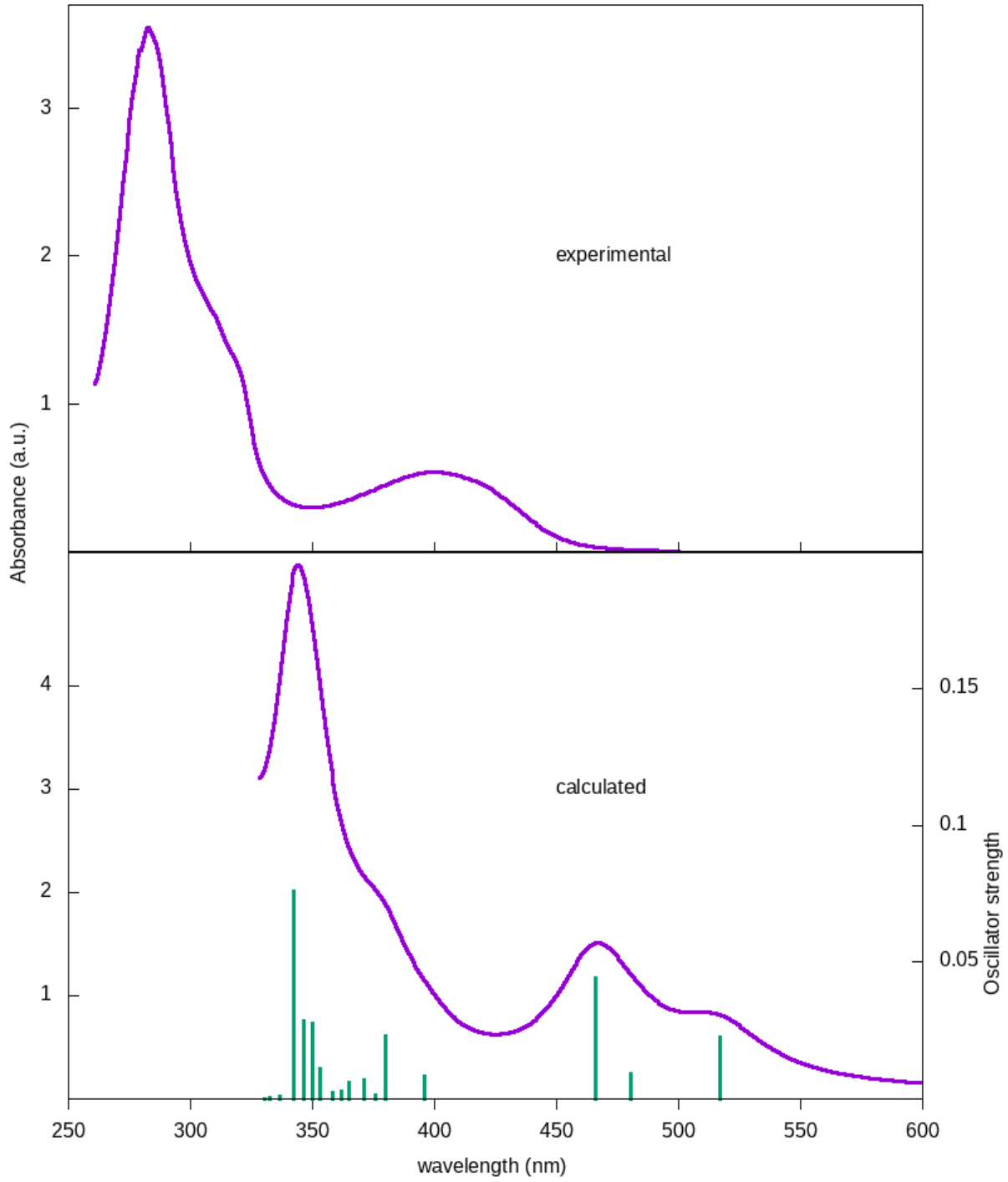

Figure S10. Experimental (top) and calculated (with the "turbo_lanczos" program, bottom) absorption spectra for complex **6**. The vertical bars in the simulated spectrum are the calculated transitions (with the "turbo_davidson" code), with height equal to the oscillator strength.

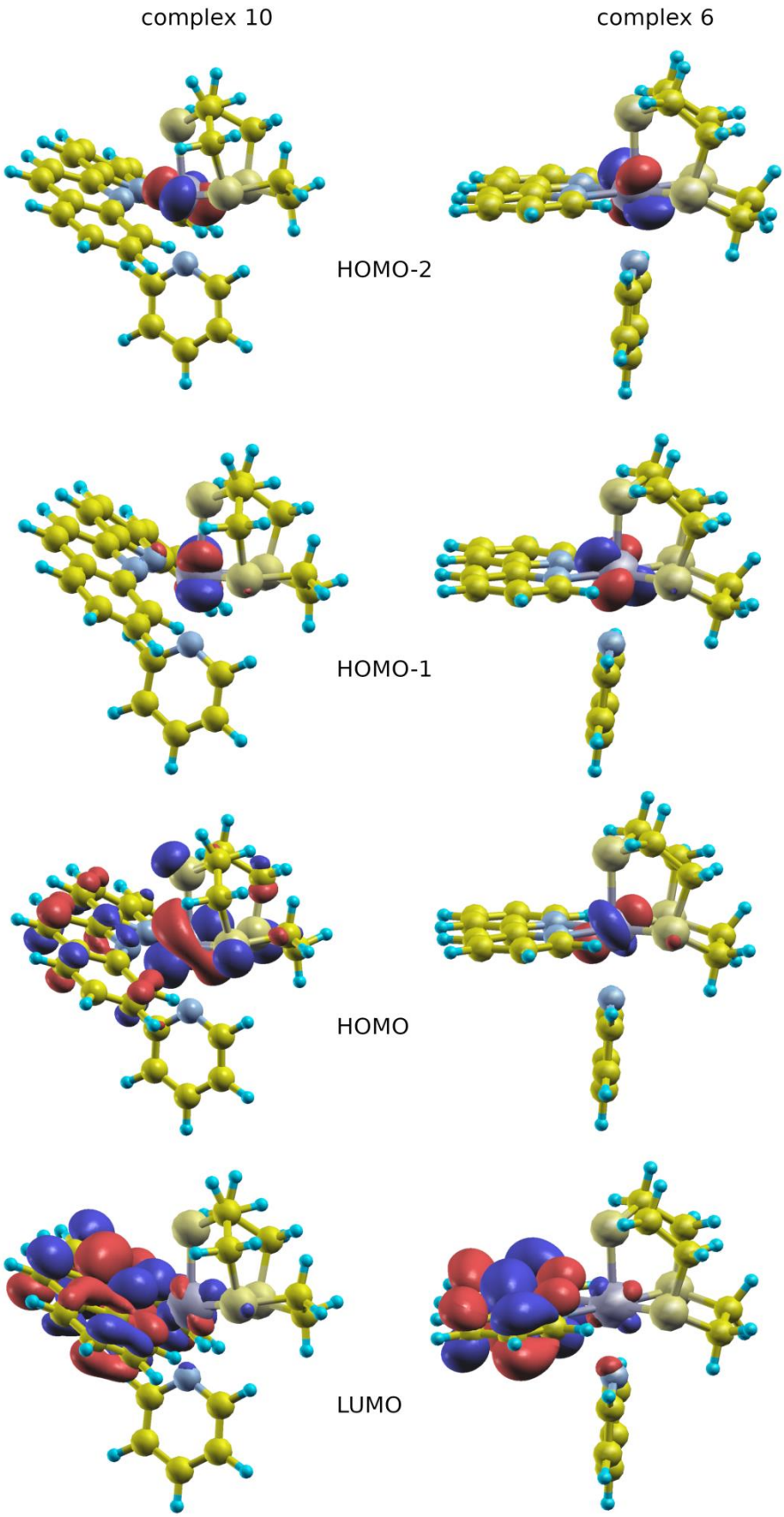

Figure S11. Selected molecular orbitals for **6** (right) and **10** (left) in the singlet ground state.

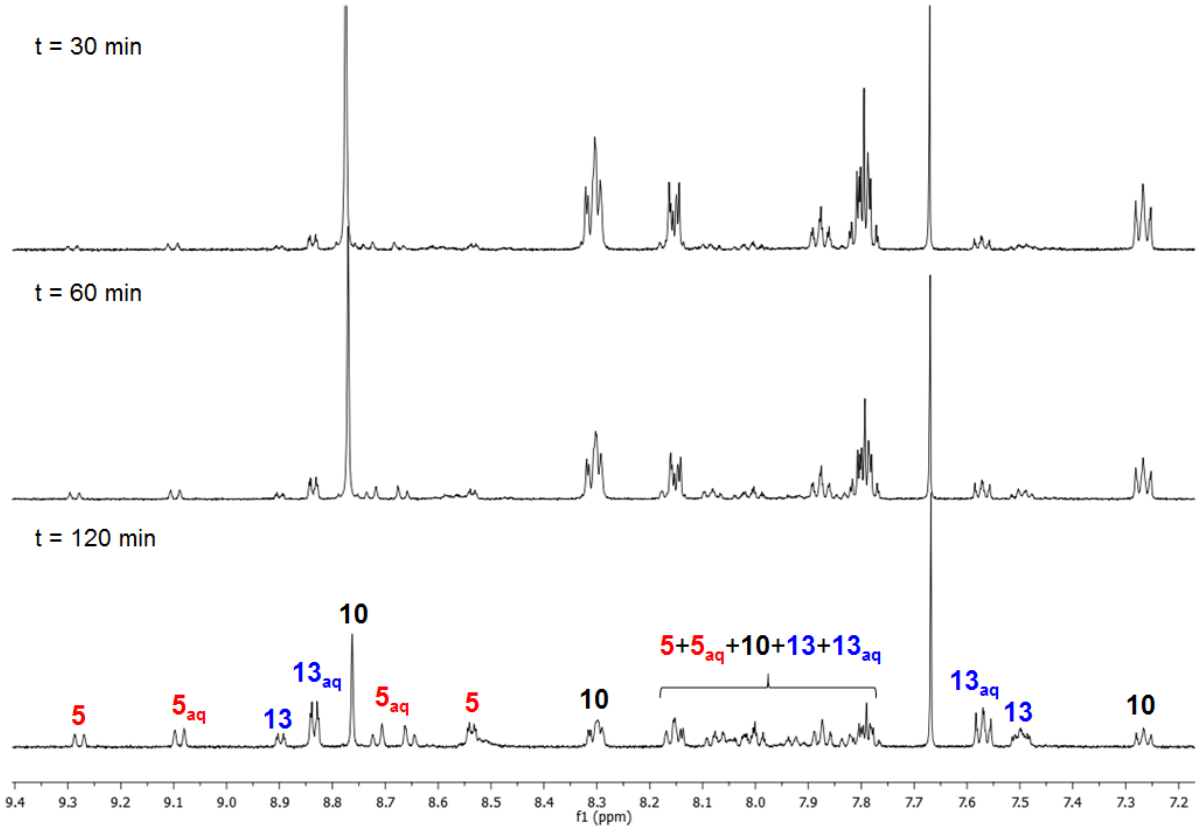

Figure S12. ^{1}H NMR spectrum in D_2O of [Ru([9]aneS_3)(bq)(py)]Cl_2 (**10**) after 30 min (top), 60 min (middle) and 120 min (bottom) of irradiation (λ = 470 nm, 40 mW).

Table S1. Selected TDDFT singlet transitions for complex **10**. Only contributions ≥ 2% are reported.

Energy (eV)	Wavelength (nm)	Oscillator strength	Major contributions	
2.2707	546	0.1006	HOMO→LUMO	84%
			HOMO–1→LUMO	12%
			HOMO–1→LUMO+1	2%
2.7264	455	0.0052	HOMO–3→LUMO	88%
			HOMO–4→LUMO	5%
			HOMO–1→LUMO	2%
2.9608	419	0.0147	HOMO→LUMO+1	63%
			HOMO–4→LUMO	17%
			HOMO–5→LUMO	7%
			HOMO–1→LUMO+1	5%
			HOMO–3→LUMO	3%
3.0767	403	0.0537	HOMO→LUMO+2	41%
			HOMO–1→LUMO+1	25%
			HOMO→LUMO+1	12%
			HOMO–4→LUMO	11%
			HOMO–1→LUMO+2	7%
3.0881	401	0.0542	HOMO–1→LUMO+1	59%
			HOMO→LUMO+2	15%
			HOMO–1→LUMO+2	7%
			HOMO→LUMO+3	6%
			HOMO–5→LUMO	4%
			HOMO–4→LUMO	2%
3.1606	392	0.1629	HOMO→LUMO+2	35%
			HOMO–4→LUMO	20%
			HOMO→LUMO+1	17%
			HOMO–1→LUMO+5	7%
			HOMO–5→LUMO	6%
			HOMO–1→LUMO+3	5%
			HOMO–1→LUMO+2	3%
3.2265	384	0.0863	HOMO–1→LUMO+2	66%
			HOMO→LUMO+4	9%
			HOMO→LUMO+3	8%
			HOMO–4→LUMO	5%
			HOMO–1→LUMO+3	3%
			HOMO→LUMO+2	2%
			HOMO→LUMO+1	2%
3.2706	379	0.0298	HOMO→LUMO+3	73%
			HOMO→LUMO+4	9%
			HOMO–1→LUMO+3	3%
			HOMO–5→LUMO	2%
			HOMO–1→LUMO+5	2%
			HOMO–1→LUMO+4	2%
			HOMO–1→LUMO+1	2%
			HOMO→LUMO+2	2%
3.3145	374	0.0278	HOMO–1→LUMO+3	61%
			HOMO→LUMO+4	16%

			HOMO–1→LUMO+2 6% HOMO–2→LUMO+1 5% HOMO–3→LUMO+1 3% HOMO→LUMO+2 2%
3.3646	368	0.0106	HOMO–2→LUMO+1 63% HOMO→LUMO+4 24% HOMO–1→LUMO+5 6% HOMO→LUMO+3 2%
3.3961	365	0.0147	HOMO–1→LUMO+4 42% HOMO–2→LUMO+1 15% HOMO–3→LUMO+1 13% HOMO→LUMO+4 13% HOMO→LUMO+3 4% HOMO–1→LUMO+3 3% HOMO–1→LUMO+2 2% HOMO→LUMO+5 2%
3.4274	362	0.0245	HOMO→LUMO+5 36% HOMO–1→LUMO+4 16% HOMO→LUMO+4 14% HOMO–2→LUMO+1 10% HOMO–1→LUMO+3 10% HOMO–5→LUMO+1 3%
3.4543	359	0.0336	HOMO→LUMO+5 52% HOMO–1→LUMO+4 17% HOMO–1→LUMO+3 7% HOMO→LUMO+4 5% HOMO–4→LUMO+1 4% HOMO–1→LUMO+5 3% HOMO–2→LUMO+2 2%
3.5194	352	0.1029	HOMO–1→LUMO+5 39% HOMO–2→LUMO+2 38% HOMO–2→LUMO+3 5% HOMO–4→LUMO 4% HOMO→LUMO+4 3% HOMO–3→LUMO+5 2%
3.5475	349	0.0652	HOMO–2→LUMO+2 41% HOMO–1→LUMO+5 27% HOMO–2→LUMO+3 8% HOMO–3→LUMO+2 6% HOMO–3→LUMO+1 4% HOMO–4→LUMO 2% HOMO–3→LUMO+3 2%

Table S2. Crystallographic data and refinement details for compounds [Ru([9]aneS$_3$)(phen)(py)]Cl$_2$·EtOH (**7**), [Ru([9]aneS$_3$)(bq)(py)]Cl$_2$ (**10**), *trans*-RuCl$_2$(bq)(CO)$_2$·2CHCl$_3$ (**11**), and [Ru([9]aneS$_3$)(bq)(NH$_3$)]Cl$_2$·CH$_3$OH (**12**).

	7	**10**	**11**	**12**
Empirical Formula	$C_{23}H_{25}N_3Cl_2RuS_3 \cdot C_2H_6O$	$C_{33}H_{41}N_3Cl_2O_2RuS_3$	$C_{20}H_{12}N_2Cl_2O_2Ru \cdot 2CHCl_3$	$C_{24}H_{27}N_3Cl_2RuS_3 \cdot CH_3OH$
Formula weight (Da)	657.68	779.84	723.02	657.67
Temperature (K)	100(2)	100(2)	100(2)	100(2)
Wavelength (Å)	0.700	0.700	0.700	0.700
Crystal system	monoclinic	triclinic	triclinic	orthorhombic
Space Group	*P* 21/n	*P* –1	*P* –1	*P* b c a
a (Å)	13.000(3)	10.420(2)	12.385(2)	12.191(1)
b (Å)	11.300(2)	10.8910(3)	13.1560(6)	20.615(2)
c (Å)	18.140(4)	16.0850(6)	16.7690(4)	21.459(1)
α (°)	90	90.229(2)	88.034(2)	90
β (°)	94.23(3)	97.034(6)	95.022(9)	90
γ (°)	90	110.666(7)	99.489(6)	90
V (Å^3)	2658(1)	1692.9(3)	2684.0(4)	5393.0(8)
Z	4	2	4	1
ρ (g·cm^{-3})	1.644	1.530	1.789	1.620
F(000)	1344	804	1424	2688
μ (mm^{-1})	0.996	0.796	1.329	0.981
θ min, max (°)	2.355, 28.351	1.258, 29.083	1.201, 28.650	1.869, 28.649
Resolution (Å)	0.74	0.72	0.73	0.73
Total refl. collctd	39653	86846	132398	88482
Independent refl.	6243	9489	14368	7202
Obs. Refl. [Fo>4σ(Fo)]	5585	9486	14345	7141
I/σ(I) (all data)	23.6	79.66	82.36	63.62
I/σ(I) (max res)	10.4	69.17	65.37	54.32
Completeness (all data)	0.919	1.000	0.994	0.989
R_{merge} (all data)	4.2%	2.6%	2.2%	2.9%
R_{merge} (max res)	7.6%	2.3%	2.1%	3.2%
Multiplicity (all data)	6.1	9.2	9.2	11.8

Multiplicity (max res)	6.1	8.2	8.3	11.6
Data/restraint/parameters	6243/0/316	9489/0/399	14368/0/632	7202/6/331
GooF	1.046	0.961	0.989	0.983
R[I>2.0σ(I)],[a] wR2 [I>2.0σ(I)][a]	0.0327, 0.0846	0.0249, 0.0742	0.0335, 0.0926	0.0225, 0.0678
R (all data),[a] wR2 (all data)[a]	0.0377, 0.0881	0.0249, 0.0742	0.0335, 0.0926	0.0227, 0.0680

[a] $R_1 = \Sigma\, ||Fo|-|Fc|| \,/\, \Sigma|Fo|$, $wR_2 = [\Sigma\, w\,(Fo^2 - Fc^2)^2 \,/\, \Sigma w\,(Fo^2)^2]^{½}$

Table S3. Selected coordination distances (Å) and angles (°) for [Ru([9]aneS_3)(phen)(py)]Cl_2·EtOH (**7**).

Bond distances (Å)			
Ru1–N11	2.138(2)	Ru1–S31	2.3129(9)
Ru1–N21	2.094(2)	Ru1–S32	2.3068(9)
Ru1–N22	2.106(2)	Ru1–S33	2.3060(9)
Bond angles (°)			
N11–Ru1–S31	178.11(6)	N22–Ru1–N11	90.63(8)
N11–Ru1–S32	90.10(6)	N22–Ru1–S31	88.90(6)
N11–Ru1–S33	92.67(6)	N22–Ru1–S32	97.81(6)
N21–Ru1–N11	87.66(8)	N22–Ru1–S33	173.36(5)
N21–Ru1–N22	79.31(8)	S32–Ru1–S31	88.15(3)
N21–Ru1–S31	94.06(6)	S33–Ru1–S31	87.98(3)
N21–Ru1–S32	176.32(5)	S33–Ru1–S32	87.95(3)
N21–Ru1–S33	95.06(6)		

Table S4. Selected coordination distances (Å) and angles (°) for [Ru([9]aneS_3)(bq)(py)]Cl_2 (**10**).

Bond distances (Å)			
Ru1–N11	2.121(1)	Ru1–S21	2.3221(3)
Ru1–N31	2.116(1)	Ru1–S22	2.3113(3)
Ru1–N32	2.107(1)	Ru1–S23	2.3178(5)
Bond angles (°)			
N11–Ru1–S21	95.37(3)	N32–Ru1–N31	76.74(4)
N11–Ru1–S22	177.17(3)	N32–Ru1–S21	99.14(3)
N11–Ru1–S23	93.36(3)	N32–Ru1–S22	88.00(3)
N31–Ru1–N11	92.78(4)	N32–Ru1–S23	173.52(3)
N31–Ru1–S21	170.91(3)	S22–Ru1–S21	87.28(1)
N31–Ru1–S22	84.51(3)	S22–Ru1–S23	87.82(1)
N31–Ru1–S23	97.93(3)	S23–Ru1–S21	85.61(1)
N32–Ru1–N11	90.59(4)		

Table S5. Selected coordination distances (Å) and angles (°) for *trans*-$RuCl_2(bq)(CO)_2 \cdot 2CHCl_3$ (**11**).

Bond distances (Å)			
Ru1–C11	1.900(2)	Ru1–Cl12	2.4095(5)
Ru1–C12	1.892(2)	Ru1–N11	2.144(2)
Ru1–Cl11	2.3837(5)	Ru1–N12	2.139(2)
Ru2–C21	1.899(2)	Ru2–Cl22	2.4179(5)
Ru2–C22	1.897(2)	Ru2–N21	2.139(2)
Ru2–Cl21	2.3858(5)	Ru2–N22	2.136(2)
Bond angles (°)			
C11–Ru1–Cl11	87.07(6)	C12–Ru1–N12	97.39(7)
C11–Ru1–Cl12	97.16(6)	Cl11–Ru1–Cl12	174.677(2)
C11–Ru1–N11	99.09(7)	N11–Ru1–Cl11	86.55(4)
C11–Ru1–N12	172.65(7)	N11–Ru1–Cl12	89.58(4)
C12–Ru1–C11	86.26(8)	N12–Ru1–Cl11	86.89(4)
C12–Ru1–Cl11	85.20(6)	N12–Ru1–Cl12	88.65(4)
C12–Ru1–Cl12	98.27(6)	N12–Ru1–N11	76.37(6)
C12–Ru1–N11	169.92(7)		
C21–Ru2–Cl21	86.33(7)	C22–Ru2–N22	98.42(7)
C21–Ru2–Cl22	97.17(7)	Cl21–Ru2–Cl22	174.19(2)
C21–Ru2–N21	99.30(7)	N21–Ru2–Cl21	85.84(4)
C21–Ru2–N22	172.41(8)	N21–Ru2–Cl22	89.01(4)
C22–Ru2–C21	84.99(8)	N22–Ru2–Cl21	87.14(4)
C22–Ru2–Cl21	85.96(6)	N22–Ru2–Cl22	89.03(4)
C22–Ru2–Cl22	98.94(6)	N22–Ru2–N21	76.34(6)
C22–Ru2–N21	170.48(7)		

Table S6. Selected coordination distances (Å) and angles (°) for [Ru([9]aneS_3)(bq)(NH_3)]Cl_2 (**12**).

Bond distances (Å)			
Ru1–N1	2.164(1)	Ru1–S31	2.3121(4)
Ru1–N21	2.135(1)	Ru1–S32	2.3341(4)
Ru1–N22	2.100(1)	Ru1–S33	2.3277(3)
Bond angles (°)			
N1–Ru1–S31	176.39(3)	N22–Ru1–N21	77.03(4)
N1–Ru1–S32	96.04(3)	N22–Ru1–S31	89.19(3)
N1–Ru1–S33	93.90(3)	N22–Ru1–S32	95.44(3)
N21–Ru1–N1	93.41(4)	N32–Ru1–S33	176.65(3)
N21–Ru1–S31	83.10(3)	S31–Ru1–S32	87.29(1)
N21–Ru1–S32	167.83(3)	S31–Ru1–S33	87.72(1)
N21–Ru1–S33	101.28(3)	S33–Ru1–S32	85.72(1)
N22–Ru1–N1	89.11(4)		